Solar Energy 194 (2019) 581–588

Contents lists available at ScienceDirect

Solar Energy

journal homepage: www.elsevier.com/locate/solener

Newly developed thermoplastic polyolefin encapsulant–A potential candidate for crystalline silicon photovoltaic modules encapsulation

Baloji Adothu[a,b,*], Parth Bhatt[c], Shashwata Chattopadhyay[a], Sarita Zele[a], Jeroen Oderkerk[d], H.P. Sagar[b], Francis Reny Costa[d], Sudhanshu Mallick[a,b,*]

[a] The National Centre for Photovoltaic Research and Education (NCPRE), Indian Institute of Technology Bombay, Mumbai, Maharashtra 400076, India
[b] Metallurgical Engineering and Materials Science, Indian Institute of Technology Bombay, Mumbai, Maharashtra 400076, India
[c] Waaree Energies Ltd., Plot 231-236, Surat Special Economic Zone, Sachin, Surat, Gujarat 394230, India
[d] Borealis Polyolefin GmbH, St.-Peterstraße 25, A-4021 Linz, Austria

ARTICLE INFO

Keywords:
Encapsulant
Ethylene-vinyl-acetate
Non-crosslinking
Thermoplastic polyolefin
Photovoltaic module

ABSTRACT

Thermoplastic polyolefin (TPO) is a newly developed non-crosslinking material for photovoltaic (PV) module lamination as an alternative to ethylene–vinyl-acetate (EVA) encapsulant. This article assesses its applicability as an encapsulant material. We report the results of various characterization tests for discoloration, optical, and thermal properties degradation before and after the UV accelerated test. To evaluate its weathering stability, the UV-365 acceleration test has been conducted on the glass to glass TPO laminate, with EVA as a benchmark. In 50 days of weatherability tests, the transmittance of EVA significantly reduced while TPO remained almost unchanged. The discoloration of TPO is around nine times slower than that of EVA. The analytical tools like Raman spectroscopy, fluorescent imaging, and spectra have been used to assess the degradation behavior, which indicates a clear difference between EVA and TPO based encapsulant. Thermal properties (glass and melt transitions) of TPO and EVA have been studied through heat-cool-heat cycle testing by differential scanning calorimeter (DSC). This test confirmed that TPO thermal properties remain almost unchanged, whereas EVA shows significant changes after 50 days of UV exposure. In the thermogravimetry analysis (TGA) results, we found that TPO is stable till a significantly higher temperature than EVA. Additionally, the 180° peel adhesion test suggests that TPO has a higher adhesion strength than EVA. This work will help in understanding the applicability of newly developed non-crosslinking TPO as a potential replacement for EVA for the PV modules.

1. Introduction

Solar photovoltaic (PV) deployment has grown at a rapid pace worldwide in the last decade. The long-term reliability of PV module depends on the effectiveness of the module packaging materials like the encapsulant and backsheet, in protecting the solar cells from the outside environment. The main components of the crystalline silicon PV module are the top glass, front-side polymeric encapsulant, solar cells, backside polymer encapsulant, and a polymeric back-sheet. In the PV module, the primary functions of the encapsulant layers are to provide high optical coupling, mechanical support, electrical isolation to the solar cells and cell circuit components (de Oliveira et al., 2018; Czanderna and Pern, 1996).

EVA has dominated the PV industry as the encapsulant of choice but numerous studies from late 1990s till today report that PV module performance reduces due to the degradation of the EVA encapsulant like browning/yellowing (which reduces the light reaching the solar cells), moisture absorption and acetic acid formation (which causes corrosion of metallization), and delamination and bubble formation in the EVA. Due to the discoloration, the transmittance of EVA film is decreased, which ultimately results in a drop in PV module power output. Various other encapsulants like silicone, ionomer, polyvinyl butyral (PVB), and polyolefin elastomers (POE), thermoplastic polyurethane (TPU) are also known in the industry as alternatives to EVA, but most often they are either very expensive or have concerns over long term-stability (Hasan and Arif, 2014). Besides, most of these alternative encapsulants need a cocktail of chemicals like multiple stabilizers, additives, peroxide curing agent, UV absorbers, etc. to function properly (Cornelia and Hädrich Ingrid). The crosslinking encapsulants, like EVA, always require organic peroxides as a curing agent to initiate

* Corresponding author at: Particulate Materials Laboratory, Department of Metallurgical Engineering and Materials Science, Indian Institute of Technology Bombay, Mumbai, Maharashtra 400076, India. Tel.: +91 22 2576 7641.
E-mail addresses: baloji@iitb.ac.in (B. Adothu), mallick@iitb.ac.in (S. Mallick).

https://doi.org/10.1016/j.solener.2019.11.018
Received 3 July 2019; Received in revised form 30 October 2019; Accepted 4 November 2019
Available online 12 November 2019
0038-092X/

the cross-linking reaction. This crosslinking ensures stability to final laminates and also helps to get proper adhesion of the encapsulant film with backsheet and glass (Kempe). The final product quality and properties depend upon the degree of crosslinking of the encapsulant, which depends on crosslinking time, lamination temperature and peroxide concentration in the encapsulant formulation (Hirschl, 2013). In the case of thermoplastic polyolefin (TPO) based encapsulants, this crosslinking step is not needed as the encapsulant usually has a higher melting temperature, which is sufficient to give necessary stability to the PV module. The avoidance of crosslinking steps offers two distinct benefits; first, all the chemicals needed for crosslinking and also crosslinking reaction by-products can be eliminated, and secondly, lamination cycle time can be significantly reduced by eliminating curing time usually needed for crosslinking encapsulants.

The scientific community started to develop a thermoplastic non-crosslinking encapsulant to overcome the above-stated problems. Discoloration, absorption of water vapor or moisture and corrosion of metallization occurs over a period of time due to the development of polymer chain conjugation, acetic acid formation, and volatiles trapping during the crosslinking reaction (Pern, 1996). Thermoplastic polyolefin (TPO) encapsulants are of two categories: crosslinking and non-crosslinking (Cornelia and Hädrich Ingrid). Non-crosslinking TPO is a new encapsulant material. No peroxide crosslinking agent is needed to ensure strong and stable laminates during the PV module lamination. Therefore, gel content or crosslinking density is always zero for non-crosslinking TPO encapsulant. Non-crosslinking TPO provides an opportunity to avoid all negative effects associated with peroxide assisted crosslinking process. So non-crosslinking TPO can become an alternative candidate to the conventional encapsulants. Due to the non-crosslinking nature, the physical properties of TPO do not change much on lamination whereas, for EVA, there is a dramatic change in the properties due to its curing reactions (Jaunich et al., 2016). TPO encapsulant is simply melted and simultaneously pressure applied to make intimate contact with the module components during lamination.

There are very few reports available on thermoplastic polyolefin elastomer (POE), specifically on TPO encapsulant. M.C. López-Escalante et al. reported that TPO is a good alternative candidate for EVA to avoid the potential induced degradation in crystalline Si PV modules because of its high volume resistivity (López-Escalante et al., 2016). B. Ottersbock et al. studied the different microclimate effects on the aging behavior of TPO and compared with EVA and concluded that there is no significant change in transmittance, yellowness value, and oxidation index of TPO encapsulant (Oreski et al., 2017). M. D. Kempe et al. studied the field testing of TPO and EVA encapsulants creep behavior in high-temperature installation sites. They concluded that the non-crosslinking thermoplastic is unlikely to result in creep in the vast majority of installations (Kempe, 2015).

An encapsulant material should satisfy the minimum criteria required in the PV module application. A new encapsulant should have minimum 90% light transmittance, high adhesion strength (> 75 N/cm), low glass transition temperature (T_g) around −40 °C, high melt transition temperature (T_m) up to 100 °C, low crystallinity (< 20%) and high thermal stability (> 300 °C). High optical transmittance helps the solar cell to capture more photons, which can lead to higher power output in the PV module. Very low T_g can eliminate the brittle failure/delamination problems when a PV module reaches an extremely low temperature of −40 °C (Agroui et al., 2012). Melt transition (T_m) defines the melting point (T_{mp}) and the melting behavior of encapsulant. High crystallinity polymers usually become brittle and hard. Due to this reason, a low crystallinity is recommended for encapsulant material. This allows more flexibility/deformation and high mechanical impact resistance in the encapsulant (Czanderna and Pern, 1996). Thermal stability is related to the thermal decomposition temperature. Thermal decomposition temperature is the temperature where the actual weight loss (chemical reaction) takes place in the encapsulant (Pern and Czanderna, 1992). A higher adhesion strength can prevent moisture ingress and can also avoid the delamination in the PV module. Low Young's modulus (< 50 MPa) is required for encapsulant film to dissipate the generated thermal stresses in the PV module (Czanderna and Pern, 1996; Agroui and Collins, 2014). In the PV industry, even the most diligent module producers may miss the deeper insight of the material behavior of encapsulant film properties simply because resin and recipe providers often act as mere raw material suppliers in the whole value chain. This study pools expertise of module producer, encapsulant manufacturer, and an independent PV research institute under one umbrella to understand the inherent properties of newly developed non-crosslinking TPO encapsulant as a potential replacement for EVA.

This article shows the strength of TPO as a new alternative to EVA as an encapsulant material. We used the UV-365 accelerated aging test to gauge its weather stability. Also, we used a heat-cool-heat cycling test to determine the thermal properties like glass and melt transitions, and the degree of crystallinity of TPO and EVA encapsulant before and after the UV exposure, which is conventionally obtained using single-stage heating test. These tests, along with early-stage discoloration detecting fluorescence imaging and spectra, gives substantial proof for TPO to be a better alternative to EVA.

2. Materials and experimental methodology

2.1. Encapsulant laminates preparation

TPO encapsulant used in the current study is Quentys BPO-8828F (0.5 mm thickness) supplied by Borealis Polyolefine GmbH. ARC coated tempered textured solar glass (SG) supplied by Gujarat Borosil Ltd (3.2 mm thickness, 300 mm × 350 mm) and a backsheet whose structure is polyvinyl fluoride (PVF or Tedlar)/polyethylene terephthalate (PET)/Primer (i.e., Tedlar/PET/Primer) manufactured by Coveme (model no.:dyMate KL 50/250) have been used for the 180° peel test. Commercially available fast-cure type EVA (0.45 mm thickness) encapsulant, backsheet, solar glass, laminator has been provided by Waaree Energies Ltd. Surat, Gujarat, India.

Four types of samples have been used throughout the study. Fig. 1(a) shows the quartz glass (QG)/encapsulant/QG structure, which has been used for the optical properties test. Fig. 1(b) shows the SG/two-layer encapsulant/ polymer backsheet structure, used for the peel adhesion test with respect to the glass. Fig. 1(c) shows the backsheet/two-layer encapsulant/backsheet structure has been used for the peel

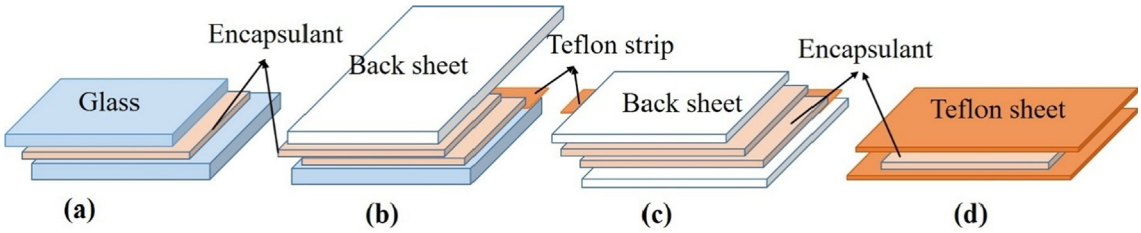

Fig. 1. Laminates structure: (a) For transmittance and reflectance test, (b) and (c) For peel adhesion test with respect to glass and with respect to backsheet, (d) For bare encapsulant film thermal and mechanical properties test.

adhesion test with respect to the backsheet. Fig. 1(d) shows the Teflon/encapsulant/Teflon structure, which has been used for the bare film thermal properties study, the encapsulant film is removed from the Teflon sheet after the lamination. The lamination has been done at 152 °C for 170 s, 20 s, and 390 s for evacuation, pressure buildup, and pressure holding (90 kPa) times, respectively for TPO encapsulant. EVA lamination has been done at 152 °C for 300 s, 20 s, and 500 s for evacuation, pressure buildup, and pressure holding (100 kPa) times, respectively. All the above laminates are prepared in an automatic industrial laminator (Boost Solar, BSL22360AC-II & III laminator).

2.2. UV weatherability test

The UV stability of the two encapsulants has been studied in a UV-365 accelerating test chamber at the National Centre for Photovoltaic Research and Education (NCPRE). Two-layer of TPO and EVA encapsulated in glass to glass laminates have been used, since it mirrors the standard architecture of a PV module. The UV-365 has a 365 nm LED-based light source (make: Thorlabs, model: SOLIS-365C, with an optical output of 3 Watts) and has the maximum light intensity of ca. 900 W/m^2. The UV-365 accelerating test has been carried out at 90° C and 10–13% RH with its maximum light intensity, in a nitrogen atmosphere for 50 days. Within 50 days, light yellow color was observed on EVA laminate (EVA), so the experiment was concluded and analyzed. For this experiment, high temperatures and low humidity have been selected because the PV modules undergo fast discoloration and delamination in hot and dry conditions (Sinha et al., 2016; Chattopadhyay, 2014). Generally, Xenon light sources have a broader range of wavelengths but they do not offer high irradiance intensity, and it takes several months to year to observe clear visible degradation/discoloration in encapsulated laminates/ in a PV module. The UV-365 chamber offers a sample heating system and as well as high irradiance intensity (ca. 900 W/m^2). Hence it takes only a few weeks to observe the clear degradation/discoloration behavior of encapsulant material.

2.3. Characterization techniques

The optical transmittance and reflectance of TPO and EVA were measured with glass to glass laminates using UV/Vis spectrophotometer (make: Jasco, model: V-650 Series) in transmittance and reflectance mode. The UV/Vis measurement has been conducted by placing them on the integrating sphere. The optical transmittance and reflectance were measured from 200 nm to 900 nm with a 1 nm step-size at average integrating time of 0.1 s. To reduce the error in measurements, the air is used for baseline correction, and glass has been used as a reference. Yellowness Index (YI) has been measured using a portable colorimeter (make: Testronix, model: TP110). This colorimeter has a 10° observer angle, and a D65 light source and its white and dark calibration have been done before the YI measurement.

The fluorescence spectra have been measured by using a silicon detector based fiber optic spectrometer (make: Research-India, model: RISC). The UV-365 nm light (make: Thorlabs, model: SOLIS-365C, with an optical output of 3 Watts) is used as a light source in fiber optic spectrometer. The light intensity has been calibrated with a standard white reflectance sample plate (made of PTFE) at 25,000 counts, 1 ms integration time, boxcar set at three and an average of 30 scans is saved. Fluorescence spectra of the sample were measured using UV-365 excitation of 25,000 counts, with 200 ms of integration time, boxcar set at three and an average of 30 scans is saved. All measurements were taken before and after the 50 days UV-365 acceleration test on TPO and EVA laminates. Fluorescence images have been captured by using the digital camera under the illumination of UV-365 light, which is stabilized at 25,000 counts. Fluorophore fluorescence background has been taken before and after the UV accelerated test by using the Raman spectrometer. The Raman spectra have been captured by using the confocal micro-Raman spectrometer (make: Horiba Jobin Yvon, Model: HR-800UV) from 100 to 3500 cm^{-1} spectral range with a 532 nm excitation laser, 25 mW power, 50X magnification (NA 0.8, spot diameter: 811 nm), 10 s of integration time. Differential scanning calorimeter (DSC) (TA instruments, Q2000) was used to study the crystallization behavior of the two encapsulants by heating from −80 to 280 °C. Thermal decomposition and thermal stability of the encapsulant have been studied with thermogravimetry analysis (TGA) (Perkin Elmer, Diamond model) by heating from 25 to 650 °C. For both DSC and TGA, around 10 mg sample has been taken in a platinum pan under a dry stream of nitrogen (gas flow 20.0 ml/min) with a heating rate of 10 °C/min. For DSC and TGA, EVA-50 and TPO-50 sample has been removed from the corner of the laminates after 50 days of UV exposure.

For measurement of encapsulant adhesion strength, the peel test has been conducted the Instron universal tensile-test apparatus by following ASTM D 903-98 standard. A 180° and T peel test has been conducted in ambient conditions (humidity = 50 ± 2% and temperature = 23 ± 1 °C) without any accelerated aging. Peel rate of 50 mm/min has been applied for 110 mm displacement on a 10 mm width peel strip. Minimum three to five strips have been used, and an average of saturation load (N) has been taken from 10 mm to 100 mm of peel extension. For tensile testing, encapsulant film samples have been cut into 100 mm length and 15 mm width. The tensile test was conducted with the Instron universal test machine (equipped with a 2 kN load cell) at 25 °C in ambient condition with a displacement rate of 50 mm/min. The test was performed according to ASTM D 882 standard.

3. Results and discussions

3.1. Optical properties of TPO and EVA

Usually, two encapsulant layers are used in industrial PV modules production. The first layer is located between the glass and the solar cells. The second one is located between the solar cells and the backsheet. The first one should be in contact with the solar cells, and it should provide hemispherical transmittance (τ) of at least 90% at wavelengths longer than 400 nm (Czanderna and Pern, 1996). The optical transmittance of single-layered and double-layered TPO laminates as a function of wavelength is shown in Fig. 2. A comparison with a transmittance of the bare QG shows the extent of blocking of UV light in Fig. 2(a). The inset figures show the single-layered and double-layered actual TPO laminates images. In Fig. 2(b), double-layered TPO and EVA laminates transmittance have been compared before and after the UV exposure.

For encapsulant materials, there is a UV cut-off wavelength below which the transmittance is less than 10% (Miller, et al., 2013), usually between 300 nm and 400 nm, whereas for quartz glass, the transmittance is as high as 75% even at 200 nm, as shown in Fig. 2(a). Here quartz is used as a reference for comparison. There is no significant change in UV-cut-off wavelength (225 nm), transmittance (> 92%), and reflectance (~7%) in 400–900 nm wavelength range for both single and double-layered TPO laminates. On the other hand, EVA laminates show a range of UV-cut-offs because of the UV absorbers added in the formulation (Czanderna and Pern, 1996). EVA transmits 80% light, effectively from 220 to 900 nm, whereas TPO can efficiently transmit above 91% light from the UV region to the entire visible spectrum (220–900 nm) (Fig. 2(b)). This is one of the major advantages of TPO encapsulant over EVA. This behavior of TPO is at par with the recently developed highly transparent EVA for use in the PV industry which gives a gain of 1% in power output of the PV module when compared to conventional EVA encapsulants (Cordula Schmid et al., 2012).

After the fifty days of the UV acceleration test, the transmittance of EVA encapsulant decreases significantly (88%) when compared to TPO encapsulant (92%), which is shown in Fig. 2(b) and values are tabulated in Table 1. The inset figure shows the visual difference (on white background) between the TPO and EVA laminates after exposed to the

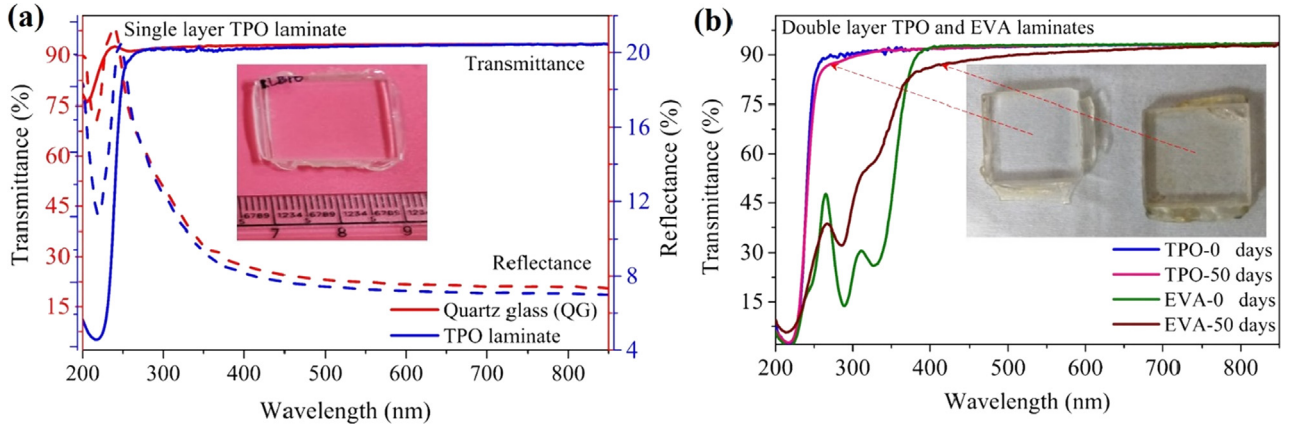

Fig. 2. (a) Optical transmittance and reflectance of single-layered TPO laminates, and (b) transmittance of double-layer laminates before and after the 50 days UV exposure.

Table 1
Transmittance and YI of TPO and EVA encapsulant before and after the UV exposure test.

Laminates	Transmittance (%)		Change in YI
	380–700 nm	220–400 nm	
TPO-0 days	92.9	85.3	0.27
TPO-50 days	92.8	83.6	0.58
EVA-0 days	93.0	40.7	0.32
EVA-50 days	88.0	53.0	5.39

UV light. The EVA developed slight yellowness in the test. In the EVA UV region, two peaks at 265 nm and 310 nm have diminished (will be lost upon further exposure), and UV radiation transmission has increased. This is due to the loss of UV absorber (Jentsch et al., 2015; Pern, 1997). Due to the loss of UV absorber, the UV radiation is absorbed by the encapsulant polymer and this results in multiple deacetylations and polyene formation (fluorophores) processes in the EVA (Czanderna and Pern, 1996), leading to EVA's faster discoloration and reduction of transmittance in the visible region (shown in Fig. 2(b)). Encapsulants having UV absorbers (having high UV-cut off wavelength) tend to undergo faster discoloration as compared to those without UV absorbers (having low UV cut-off wavelength) (Cordula Schmid et al., 2012). Since TPO is a material with low UV cut-off, there is no observable change in transmittance spectra in the UV accelerated test.

In order to confirm the discoloration, YI has been measured after the lamination, before and after UV exposure. The difference between YI value measured before UV exposure and after lamination is taken as 0 days and whereas the difference between measured YI value after lamination and after 50 days UV exposure is taken as 50 days change in YI. The change in YI is shown in Table 1. The YI data suggest that EVA undergoes nine times faster discoloration than TPO encapsulant. This discoloration is due to the fluorophores generation via multiple deacetylations leading to multiple polyenes (unsaturated bonds) formation (Czanderna and Pern, 1996). It is difficult to detect the early stage encapsulant discoloration in the visual image or through the naked eye but it is possible to detect through fluorescence imaging (Dolia et al., 2018). Since these fluorophores get excited under the UV light and emit fluorescence in the visible region. In Fig. 3, TPO laminate shows clear transparency in both visual and fluorescence images, both before and after exposure to UV-365 light. Whereas in EVA-50 days fluorescence image (Fig. 3(b)), fluorescence is observed in the central portion but the discoloration is not visible in visual images. That means, that the UV excitable fluorophores are accumulated at the central portion (yellow-brown region) of EVA-50 laminate. All the fluorescence images have been taken with a digital camera under 365 nm UV light. It is well known that in the degraded PV module, discoloration of the encapsulant is primarily seen in the center portion of the cells whereas the cell edges are dominated by photobleaching (due to the availability of oxygen along the cell edges) (Czanderna and Pern, 1996). A similar trend is observed in the EVA-50 day's sample, but there is no such trend or UV excitable fluorophores present in the TPO laminates (as shown in Fig. 3). This is a major advantage of TPO encapsulant.

In order to confirm the emission from fluorophores, fluorescence spectra have been recorded. Fluorescence spectra and Raman spectra have been recorded at the central portion of laminates, as shown in the inset figure in Fig. 4(a). Fluorescence spectra of EVA-50 days sample show the fluorophores emission within the visible region from 540 to 700 nm, and its maximum peak emission is 622 nm, which is clearly shown in the inset figure (plotted after the baseline subtraction) in Fig. 4(a). This maximum emission peak at 622 nm confirms that EVA encapsulant is discoloring with a dark orange color and is very close to the dark brown color reported by the F.J. Pern group (Pern, 1993). In TPO, there is no such emission peak observed before and after the UV exposure test. From the fluorescence intensity, fluorescence emission is nine to ten times lower than EVA, which is shown inset figure Fig. 4(a).

Typical Raman spectra show strong and sharp vibration peaks of undegraded samples. EVA and TPO shows similar strong vibrations at 1068 v(CC)), 1126 (v(CC)), 1295 (t(CH)), 1438 (d(CH)), 1724 (v(CO)), 2835 (v(CH_2), and 2895 cm^{-1} v((CH_3)) except in EVA-50 days sample. Among all these, CH_2 and CH_3 are the strong stretching vibrations in EVA and TPO, as shown in Fig. 4(b). But when EVA degrades, a strong fluorescence background will appear at 1724 cm^{-1} (CO vibration stretching) (Peike et al., 2011). Similarly, a very intense fluorescence background shown in EVA- 50 days' samples as shown in Fig. 4(b). This is due to the conjugated fluorophores such as polyenes (C═C) and α,β-unsaturated carbonyl groups ((C═O), (C−O)) generation in the EVA through the Norrish-I & Norrish-II (multi-deacetylation) reaction, and polymer chain scission mechanisms under the UV and as well as elevated temperature (Czanderna and Pern, 1996). The possible main reason for fluorophore generation in EVAs are loss of stabilizer or additive (Jentsch et al., 2015), loss of VA unit and main chain scission (Allen et al., 2000). In EVA, the VA unit (shown in the [1]red circle in the Fig. 4(b)) splits into ketones, acetic acid (deacetylation) and aldehydes & other gases (CO, and CO_2) through the Norrish-I, II, III reactions respectively. All the species have CO vibrational stretching. The corresponding fluorescence background for CO stretching vibrations appears at 1724 cm^{-1}. Simultaneously, due to the polymer main chain scission, another fluorescence background appears near the CH (CH_2 at

[1] For interpretation of color in Figs. 3 and 4, the reader is referred to the web version of this article.

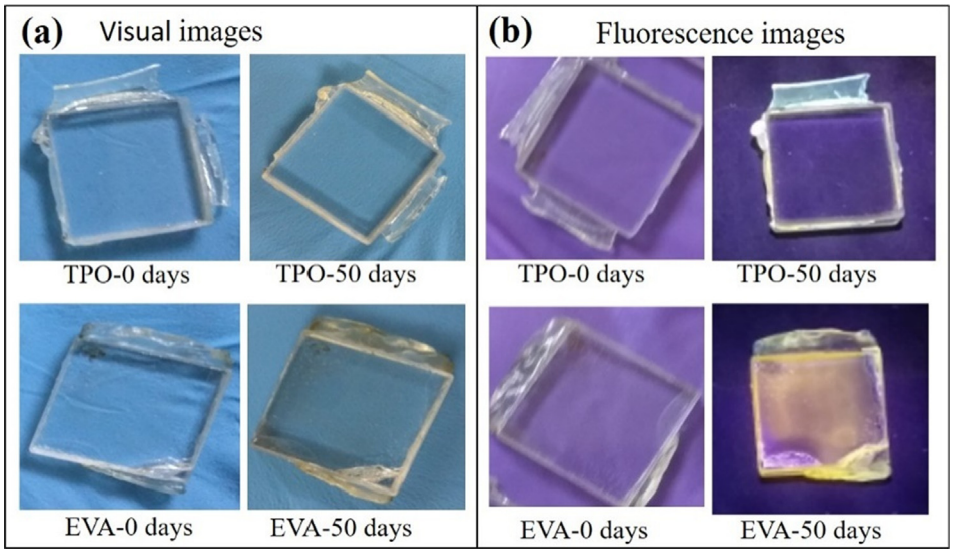

Fig. 3. (a) Visual images and (b) fluorescence image.

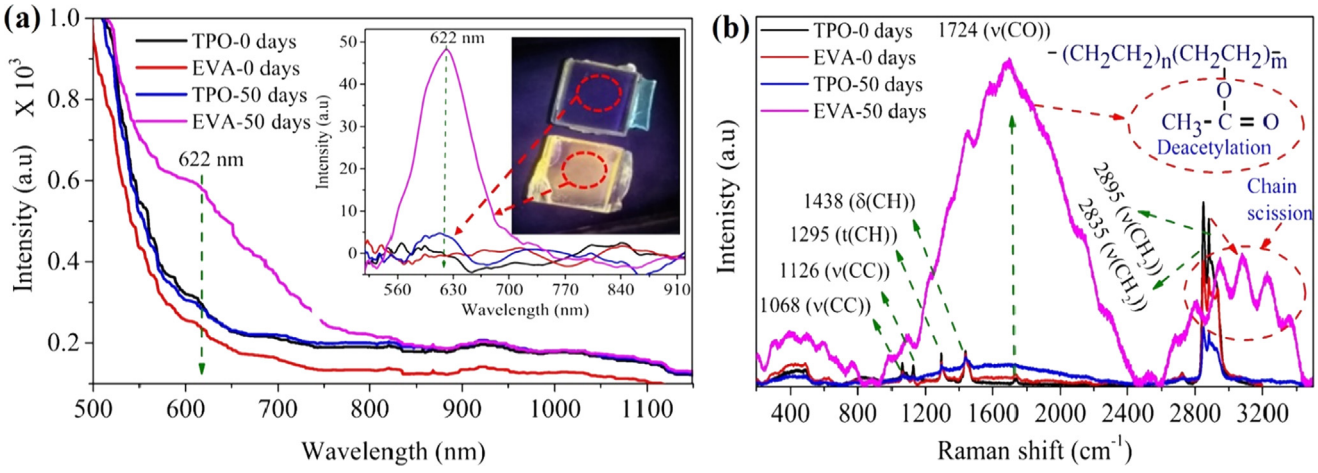

Fig. 4. (a) Fluorescence spectra and (b) Raman spectra.

$2853\,cm^{-1}$ and CH_3 at $2895\,cm^{-1}$) vibration region (shown in red circle) (Peike et al., 2011). The EVA-50 day's sample shows such behavior. But TPO does not have any such fluorophore generating VA units. Since there is no fluorescence background causing fluorophores in TPO, it shows a strong and sharp vibrational spectrum even after the UV accelerated test, indicating that TPO is more stable than EVA.

3.2. Thermal properties

From the above results, it is confirmed that TPO has better weather stability than EVA. In this section, we will discuss the thermal properties of TPO and EVA encapsulants (before & after the lamination (BL & AL) and after the UV exposure). DSC based encapsulant thermal properties are studied by the heat-cool-heat cycle for all the samples (TPO-BL & TPO-AL, EVA-AL, TPO-50 and EVA-50 days). The heat-cool-heat cycle shows the real behavior of encapsulant film when a PV module experiences the extremely low temperature ($< -40\,°C$, cold climatic zone), and extremely high temperature (85 °C, hot climatic zone). The heat-cool-heat cycle also allows understanding the complete thermal behavior and missing/eliminated thermal history of the samples. Fig. 5 shows a heat-cool-heat cycle with all transitions like T_g, T_m, T_c, and crosslinking reaction regions of all the samples. There are no significant changes observed in the DSC heat-cool-heat profile path for TPO-BL & TPO-AL, whereas in EVA-BL & EVA-AL shows the significant difference

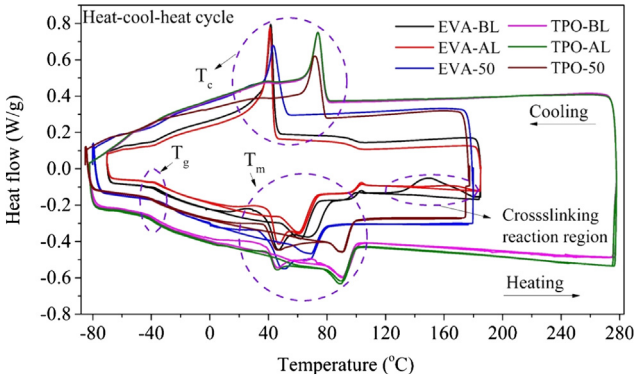

Fig. 5. DSC heat-cool-heat profile for TPO and EVA encapsulant films.

due to its crosslinking nature. In order to check the crosslinking or any phase changes in TPO, initially, the heat cool-heat cycle was done till 280 °C in both TPO-BL and TPO-AL samples. Which confirmed that there are no crosslinking reactions/phase changes involved in TPO encapsulant, which is clearly shown in Fig. 5. We already know that EVA is a crosslinking reaction-based encapsulant and its crosslinking reaction has shown to be between 125 °C and 180 °C and which is clearly matched for EVA-BL. EVA-AL also shows the crosslinking

Table 2
Thermal properties of EVA and TPO encapsulants.

Samples details	T_c °C	T_g °C	T_{mp} °C	ΔH_{mp} J/g	χ_c %
EVA-BL	42.2	−38.3	62.4	13.2	4.6
EVA-AL	40.3	−38.5	62.2	11.4	3.4
EVA-50	45.1	−32.2	70.1	27.3	9.5
TPO-BL	73.8	−43.9	91.5	22.9	7.8
TPO-AL	74.2	−44.1	92.1	18.8	6.5
TPO-50	73.6	44.3	92.3	19.7	6.8

reaction from 150 °C to 180 °C. Which means EVA-AL is not fully crosslinked. During the cooling process, a large exothermic peak appeared, which is related to the T_c of the encapsulants shown in Fig. 5. In all TPO (including UV exposed sample), EVA-BL & EVA-AL samples, the T_c position is almost unchanged, and values are tabulated in Table 2. But in EVA-50 days UV exposed sample T_c position is slightly (5 °C) shifted to the higher temperature. This indicates that the EVA T_c position can slightly change with the continuous exposure of UV radiation. But still, TPO's T_c value is > 35 °C higher than T_c of EVA, even after exposure to UV radiation.

3.2.1. Glass transition temperature

As discussed earlier, a PV module goes through temperatures as low as −40 °C, under such conditions the encapsulant should be in a rubbery flexible state and not in a glassy or brittle state in order to avoid delamination/cracks. Fig. 6 shows all the TPO samples, the T_g position is almost unchanged (−44 °C) during the first and second heating. Whereas in EVA-BL and EVA-AL samples T_g remains the same. But in EVA-50 days UV exposed sample, T_g is slightly shifted from −38 °C to −32 °C. This may be due to the fluorophores (such as carbonyl groups, saturated and unsaturated polyenes) formation (samples show strong fluorescence as depicted in Fig. 3(b) and Fig. 4). But TPO still shows −10 °C lower T_g value than EVA and is not effected even after 50 days of UV exposure. This means that TPO can show better flexibility and performance even in extremely low-temperature conditions.

3.2.2. Melting point

The melt transition region (T_m) of TPO-BL, TPO-AL, and TPO-50 days samples starts at 35 °C and ends at 105 °C, whereas in all the EVA samples T_m starts at 35 °C but ends at different temperatures shown in Fig. 7. For EVA-AL and EVA-50 days samples, T_m ends at 74 °C and 82 °C respectively. There is a 10 °C degree increment in T_m of EVA-50 days UV exposed sample. This may also be the same reason, as we discussed earlier (fluorophores generation). TPO and EVA show two endothermic reaction peaks in their T_m region. The first low-temperature endothermic peak is related to the melting of small irregular

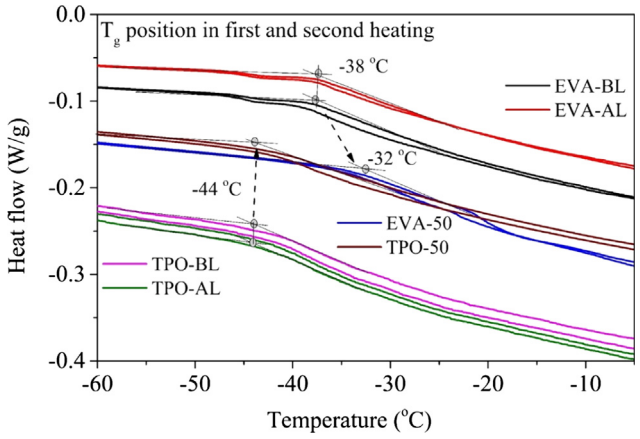

Fig. 6. Estimation of T_g for TPO and EVA encapsulant films.

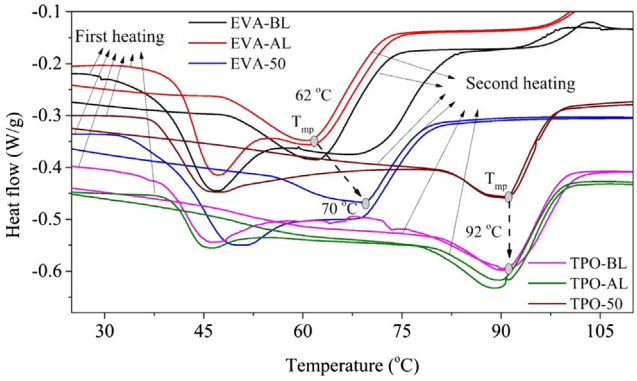

Fig. 7. Shifting of T_{mp} in the T_m region of TPO and EVA encapsulant films.

crystallite segments, and the second higher temperature endothermic peak is related to the actual melting point (T_m) of large regular crystallite segments (Agroui et al., 2012; Agroui and Collins, 2014). In second heating, the low-temperature endothermic melting peak disappears, and a high-temperature endothermic melting peak remains. That means small irregular crystallites segments are lost during the completion of fist heating, while large regular crystallites segments still exist in first and second heating. Due to this reason, a high-temperature endothermic peak is considered as the actual T_{mp} for EVA (Agroui et al., 2012; Agroui and Collins, 2014), and this is also true for TPO encapsulant.

Due to the crosslinked nature of EVA-AL, T_{mp} is slightly shifted to a lower temperature when compared to EVA-BL. Whereas in the EVA-50 sample, T_{mp} significantly shifted from 62 °C (EVA-AL) to 70 °C. This peak shifting is common for exposed/discolored EVA. This is because of the increase in the crystallinity during UV exposure (Oreski et al., 2017). But in TPO samples, T_{mp} is almost unchanged (around 92 °C) during the first heating, second heating, and even after exposure to UV for 50 days. In the hottest installation sites, the PV module is expected to reach maximum temperatures of 100 °C (Miller et al., 2010). At this maximum operating temperature, EVA is in a molten state and has a higher chance of fluorophores generation. Since TPO has high T_m, it can maintain its small fraction of crystal segments and it can prevent the mechanical creep when a PV module reaches the maximum operating temperature of 85–100 °C (Kempe, 2015). This is another major advantage of TPO encapsulant that it does not undergo fast discoloration or fluorophores generation like EVA.

3.2.3. Degree of crystallinity

DSC T_m region also provides the degree of crystallinity of encapsulants by measuring the area under the melting peak. In order to avoid the thermal history of the sample and as per the literature suggests, the degree of crystallinity has been measured only for the second heating curve. The degree of crystallinity is calculated via the total enthalpy method (Agroui et al., 2012; Agroui and Collins, 2014) according to Eq. (1):

$$\chi_C(\%) \equiv \left(\frac{\Delta H_{mp}}{\Delta H_{100}} \times 100\%\right) \quad (1)$$

where ΔH_{mp} is the specific enthalpy of melting of TPO/EVA samples and ΔH_{100} is the specific enthalpy of melting for 100% crystalline polyethylene (288 J/g). The estimated χ_c of all the samples have been tabulated in Table 2. In EVA-BL and EVA-AL samples, χ_c is almost unchanged. Whereas in EVA 50 days sample χ_c increased from 3.4% (EVA-AL) to 9.5%. This may be due to the UV radiation and as well as continuous heating during the UV exposure test. During the UV exposure, a similar increment in χ_c is also reported for EVA encapsulant (Oreski et al., 2017). VA unit loss as volatile acetic acid and increment in the degree of crosslinking can make the ethylene unit stronger during

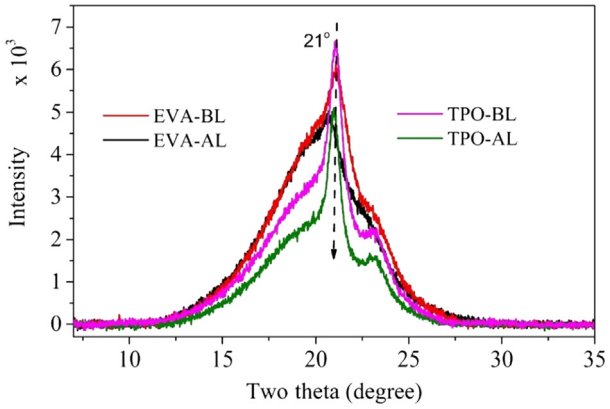

Fig. 8. XRD pattern for TPO encapsulant film.

the thermal and photothermal degradation (de Oliveira et al., 2018). These are maybe the possible reasons for a slight increment in T_c; T_g, T_m, T_{mp}, and χ_c of EVA-50 days sample. There are no such acid-generating VA units/ fluorophores generating groups in TPO. Due to this reason, TPO does not show any fluorescence (which is clearly shown in Fig. 3(b) and Fig. 4). Because of these reasons, in all the TPO samples, T_c, T_g, T_m, T_{mp}, and χ_c are almost unchanged.

There is no dramatic change in the DSC degree of crystallinity before and after the lamination and this is also in good agreement with the XRD patterns shown in Fig. 8. XRD pattern shows an amorphous phase broad peak at 21° of its two theta angle. It would be considered as a complex semi-crystalline phase involved in EVA encapsulant due to the coexistence of monomers, which is also similar for TPO (Agroui et al., 2012; Agroui and Collins, 2014). But the XRD pattern also showed that there is a slight decrease in the intensity after the lamination. The XRD pattern suggests a higher crystallinity for TPO as compared to EVA, both before and after lamination. XRD was not analyzed on 50 days exposed samples, because not enough sample film could be collected.

3.2.4. Thermal stability

Fig. 9 shows thermal stability and thermal decomposition stages of TPO and EVA encapsulants. We already know that EVA shows two-stage decomposition. The first stage degradation is due to the acetic acid evolution (deacetylation), and the second stage is due to the main chain loss (Pern and Czanderna, 1992). Fig. 9 shows that EVA is thermally stable up to 260 °C, because its first decomposition starts at 260 °C. TPO shows only single-stage decomposition at ca. 400 °C, which is due to polymer main chain loss. In a PV module due to cell defects, hot spots as small as 1 mm^2 are created and the local temperature reaches up to ca. 300 °C (Shifeng Deng et al., 2017). At this temperature, EVA undergoes significant deacetylation, but TPO can still provide better performance without decomposition up to 400 °C. It is also observed that even after UV exposure there is no change in the thermal decomposition temperatures of both EVA and TPO.

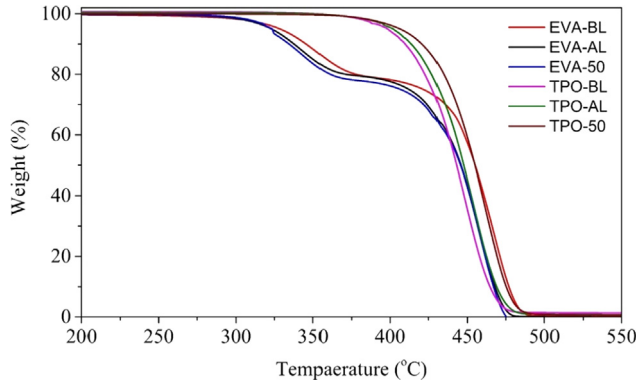

Fig. 9. TGA curves of TPO and EVA encapsulant films.

3.3. Adhesion and Young's modulus of TPO encapsulant

Peel adhesion strength is a very important property to evaluate the bonding of the different interfaces in a PV module for their longevity. Peel profile shows fluctuations, which is a generally observed phenomenon in encapsulant peel test (Wu et al., 2014; Pern and Glick, 2003). Therefore, the final peel adhesion strength has been taken from the mean of four to five repetitive peel test samples. Here TPO shows around 200 N/cm at the glass-encapsulant interface and as well as at the backsheet-encapsulant interface and which are shown in Fig. 10(a) & (b). As per reports, a standard EVA shows adhesion strength of 80–100 N/cm (Wu et al., 2014; Pern and Glick, 2003).

Fig. 11 shows the mechanical deformation behavior of TPO-BL and TPO-AL in the tensile stress vs strain curve. The elastic modulus of the TPO encapsulant has been calculated from the stress/strain-curve in the elastic region. This elastic modulus has been calculated as per ASTMD-882-02 and its R^2 value is around 0.999. It is found that Young's modulus is nearly 21 MPa & 19 MPa for TPO-BL and TPO-AL respectively. TPO encapsulant also has the same Young's modulus as EVA (20 MPa) (Czanderna and Pern, 1996).

4. Conclusion

TPO has been successfully laminated here and its properties have been evaluated for the PV module encapsulation application. Single-layered and double-layered laminates show around 92% optical transmittance. When compared with TPO, EVA-50 days laminates show a significant reduction in transmittance due to its discoloration after the UV exposure test. TPO does not show any discoloration. This is also confirmed by fluorescence imaging. Raman spectra also confirmed that the EVA-50 day's sample has a strong fluorescence background due to its discoloration, whereas in TPO, it does not show any fluorescence background. This UV weather test results confirm that TPO is a superior encapsulant than EVA. The thermal behavior of TPO and EVA encapsulant film has been studied by DSC using heat-cool-heat cyclic testing to correlated the extreme climatic conditions the PV modules may experience. It has been found that T_g, T_c, T_{mp} and χ_c almost unchanged for TPO, whereas EVA shows significant change due to the UV exposure effect. It is also found that there is no crosslinking reaction involved in TPO encapsulant. Extremely low T_g and high melting temperature ranges are the major advantages of TPO encapsulant. It would be expected that the TPO encapsulant can prevent the creep flow and can provide high mechanical strength when the PV module reaches the maximum operating temperature (85–100 °C) due to its high melt transition of 105 °C. TGA results show that TPO has only single-stage decomposition and is thermally stable up to 400 °C. Such higher thermal stability of TPO can be advantageous in the PV module to prevent encapsulant degradation from the hot spots. TPO encapsulant gives very high peel adhesion strength of more than 200 N/cm at the glass-encapsulant and backsheet-encapsulant interfaces within the shorter lamination cycle time of 9 min. Tensile stress–strain results show that TPO Young's modulus of elasticity is around 20 MPa. From all the results, it can be concluded that TPO material can become a potential candidate for the PV module encapsulation.

Declaration of Competing Interest

The authors declared that there is no conflict of interest.

Acknowledgments

The authors would like to acknowledge Borealis Polyolefine GmbH, Austria, and Waaree Energies Ltd. Surat, India, for providing materials,

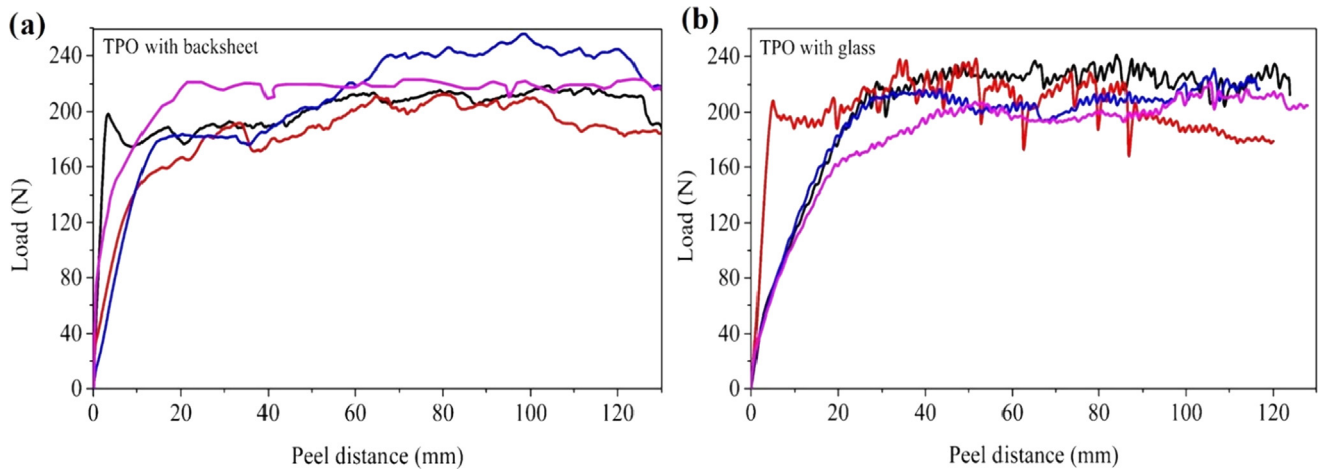

Fig. 10. Peel test profiles: (a) TPO with backsheet, (b) TPO with glass. The colors represent different identical samples.

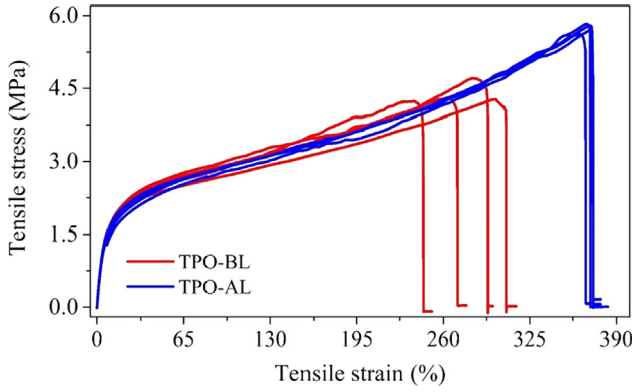

Fig. 11. Tensile stress and strain curves for TPO encapsulant film.

equipment, and support for the preparation and measurement of sample analysis during this study. We are thankful to the Metallurgical Engineering and Materials Science department, Particulate Material lab, and SAIF at IIT Bombay for the characterization facilities.

This work was supported by the NCPRE funded by the Ministry of New and Renewable Energy of the Government of India through the Project No. 31/09/2015-16/PVSE-R&D dated 15th June 2016. The authors would like to thank financial assistanship from the multi-institutional project No: Spons/MT/MS-1/2018 and dated Jun 25, 2018, by Borealis (Vienna, Austria), Waaree (Surat, India).

Appendix A. Supplementary material

Supplementary data to this article can be found online at https://doi.org/10.1016/j.solener.2019.11.018.

References

Agroui, K., Collins, G., 2014. Determination of thermal properties of crosslinked EVA encapsulant material in outdoor exposure by TSC and DSC methods. Renew. Energy 63, 741–746.

Agroui, K., Collins, G., Farenc, J., 2012. Measurement of glass transition temperature of crosslinked EVA encapsulant by thermal analysis for photovoltaic application. Renew. Energy 43, 218–223.

Allen, N.S., Edge, M., Rodriguez, M., Liauw, C.M., Fontan, E., 2000. Aspects of the thermal oxidation, yellowing and stabilisation of ethylene vinyl acetate copolymer. Polym. Degrad. Stab. 71 (1), 1–14.

Chattopadhyay, S., et al., 2014. Visual degradation in field-aged crystalline silicon PV modules in india and correlation with electrical degradation. IEEE J. Photovolt. 4 (6), 1470–1476.

Cordula Schmid, J.W., Chapon, Julien, Kinsey, Geoffrey, Bokria, Jayesh, 2012. Impact of high light transmission eva-based encapsulant on the performance of PV modules. In: 27th European Photovoltaic Solar Energy Conference and Exhibition, pp. 3494–3498.

Cornelia, W., Hädrich Ingrid, K.W. Overview of PV module encapsulation materials. Photovolt. Int., pp. 85–92.

Czanderna, A.W., Pern, F.J., 1996. Encapsulation of PV modules using ethylene vinyl acetate copolymer as a pottant: A critical review. Sol. Energy Mater. Sol. Cells 43 (2), 101–181.

Dolia, K., Sinha, A., Tatapudi, S., Oh, J., Tamizhmani, G., 2018. Early detection of encapsulant discoloration by UV fluorescence imaging and yellowness index measurements. In: 2018 IEEE 7th World Conference on Photovoltaic Energy Conversion (WCPEC) (A Joint Conference of 45th IEEE PVSC, 28th PVSEC & 34th EU PVSEC), pp. 1267–1272.

Hasan, O., Arif, A.F.M., 2014. Performance and life prediction model for photovoltaic modules: Effect of encapsulant constitutive behavior. Sol. Energy Mater. Sol. Cells 122, 75–87.

Hirschl, C., et al., 2013. Determining the degree of crosslinking of ethylene vinyl acetate photovoltaic module encapsulants - A comparative study. Sol. Energy Mater. Sol. Cells 116, 203–218.

Jaunich, M., Bohning, M., Braun, U., Teteris, G., Stark, W., 2016. Investigation of the curing state of ethylene/vinyl acetate copolymer (EVA) for photovoltaic applications by gel content determination, rheology, DSC and FTIR. Polym. Test. 52, 133–140.

Jentsch, A., Eichhorn, K.J., Voit, B., 2015. Influence of typical stabilizers on the aging behavior of EVA foils for photovoltaic applications during artificial UV-weathering. Polym. Test. 44, 242–247.

Kempe, M.D., et al., 2015. Field testing of thermoplastic encapsulants in high-temperature installations. Energy Sci. Eng. 3 (6), 565–580.

Kempe, M. Overview of Scientific Issues Involved in Selection of Polymers for PV Applications. In: 37th IEEE Photovoltaic Specialists Conefrence (PVSC 37) Seattle, Washington, pp. 1–6.

López-Escalante, M.C., Caballero, L.J., Martín, F., Gabás, M., Cuevas, A., Ramos-Barrado, J.R., 2016. Polyolefin as PID-resistant encapsulant material in PV modules. Sol. Energy Mater. Sol. Cells 144.

Miller, D.C., Kempe, M.D., Glick, S.H., Kurtz, S.R., 2010. Creep in photovoltaic modules: examining the stability of polymeric materials and components. In: 2010 35th IEEE Photovolt. Spec. Conf., pp. 262–268.

Miller, D.C., et al., 2013. Examination of an optical transmittance test for photovoltaic encapsulation materials. Natl. Renew. Energy Lab., September, pp. 1–13.

de Oliveira, M. Michele Cândida Carvalho, Cardoso Diniz, Antônia Sônia Alves, Viana, V. de F. C.L. Machado, 2018. The causes and effects of degradation of encapsulant ethylene vinyl acetate copolymer (EVA) in crystalline silicon photovoltaic modules: A review. Renew. Sustain. Energy Rev. 81, pp. 2299–2317.

Oreski, G., Pinter, G., Ottersb, B., 2017. Comparison of different microclimate effects on the aging behavior of encapsulation materials used in photovoltaic modules. vol. 138, pp. 182–191.

Peike, C., Kaltenbach, T., Weiß, K., Koehl, M., 2011. Non-destructive degradation analysis of encapsulants in PV modules by Raman Spectroscopy. Sol. Energy Mater. Sol. Cells 95, 1686–1693.

Pern, F.J., 1993. Luminescence and absorption characterization of ethylene-vinyl acetate encapsulant for PV modules before and after weathering degradation. Polym. Degrad. Stab. 41 (2), 125–139.

Pern, F.J., 1996. Factors that affect the EVA encapsulant discoloration rate upon accelerated exposure. Sol. Energy Mater. Sol. Cells 41–42, 587–615.

Pern, F., 1997. Ethylene vinyl acetate (EVA) encapsulants for photovoltaic modules: Degradation and discoloration mechanisms and formulation modifications for improved. Die Angew. Makromol. Chemie 252, 195–216.

Pern, F.J., Glick, S.H., 2003. Adhesion strength study of EVA encapsulants on glass substrates. In: The National Center for Photovoltaics and Solar Program Review Meeting; Denver, Colorado, 2003, pp. 24–26.

Pern, F.J., Czanderna, A.W., 1992. Characterization of ethylene vinyl acetate (EVA) encapsulant: Effects of thermal processing and weathering degradation on its discoloration. Sol. Energy Mater. Sol. Cells 25 (1–2), 3–23.

Shifeng Deng, Z.X., Zhang, Zhen, Ju, Chenhui, Dong, Jingbing, Xinchun Yan, G.X., Xu, Tao, 2017. Research on hot spot risk for high-efficiency solar module. Energy Procedia 130, pp. 77–86.

Sinha, A., Sastry, O.S., Gupta, R., 2016. Nondestructive characterization of encapsulant discoloration effects in crystalline-silicon PV modules. Sol. Energy Mater. Sol. Cells 155.

Wu, D., Zhu, J., Betts, T.R., Gottschalg, R., 2014. Degradation of interfacial adhesion strength within photovoltaic mini-modules during damp-heat exposure. Prog. Photovolt. Res. Appl. 22 (7), 796–809.